Synthetic Metals 161 (2011) 1892–1897

Contents lists available at ScienceDirect

Synthetic Metals

journal homepage: www.elsevier.com/locate/synmet

Electronic structure of thin film cobalt tetracyanoethylene, Co(TCNE)$_x$

E. Carlegrim [a], Y. Zhan [a], M.P. de Jong [b], M. Fahlman [a,*]

[a] Department of Physics, Chemistry and Biology, Linköping University, SE-581 83 Linköping, Sweden
[b] MESA+ Institute for Nanotechnology, University of Twente, 7500 AE Enschede, The Netherlands

ARTICLE INFO

Article history:
Received 27 September 2010
Received in revised form 14 June 2011
Accepted 20 June 2011
Available online 20 July 2011

Keywords:
Organic magnets
Photoelectron spectroscopy
Near edge X-ray absorption fine structure

ABSTRACT

V(TCNE)$_x$, TCNE = tetracyanoethylene, $x \sim 2$, is a semiconducting organic-based magnet and one of very few organic-based magnets with critical temperature above room temperature (RT). With the aim to understand the key design criteria for achieving RT organic-based magnets we have started to study the electronic and chemical structure of members of the M(TCNE)$_x$ family with significantly lower critical temperatures than V(TCNE)$_x$. In this paper, Co(TCNE)$_x$, $x \sim 2$, ($T_C \sim 44$ K, derived from its powder form) were prepared by a method based on physical vapor deposition, resulting in oxygen-free thin films. By using a variety of photoemission and X-ray absorption techniques the highest occupied molecular orbital (HOMO) of Co(TCNE)$_x$ was determined to mainly be TCNE$^-$-derived while the states originating from Co(3d) are localized at higher binding energies. This is in stark contrast to V(TCNE)$_x$ where V(3d) is mainly responsible for the HOMO, but in line with the results of Fe(TCNE)$_x$ ($T_C \sim 121$ K, derived from its powder form) for which the HOMO also is TCNE$^-$-derived. Moreover, the results propose Co(TCNE)$_x$ to contain large amounts of local bonding disorder in contrast to V(TCNE)$_x$ which can be grown virtually defect free. We speculate that cobalt binds to vinyl – instead of cyano groups, hence creating a disordered bonding arrangement which deviates from octahedral. The very weak (<1 eV) crystal field splitting and a large spread in the local ligand field strengths due to disorder in Co(TCNE)$_x$ are in agreement with the absence of fine structure in the Co L-edge spectra.

1. Introduction

The discovery of room temperature (RT) magnetism ($T_C \sim 400$ K) [1] in vanadium tetracyanoethylene, V(TCNE)$_x$, generated extensive interest in organic-based magnets of the M(TCNE)$_x$, M = V, Fe, Mn, Co, Ni, etc., $x \sim 2$, family [2] which recently has been extended to also include Cr, Nb and Mo [3]. V(TCNE)$_x$ is semiconducting [4] and has fully spin-polarized transport levels with the highest occupied molecular orbital (HOMO) of V(TCNE)$_x$ mainly localized on the vanadium sites while the lowest unoccupied molecular orbital (LUMO) is TCNE$^-$ derived [5,6]. The coupling between V^{2+} and the two TCNE$^-$ units is antiferromagnetic yielding a ferrimagnetic state and hence a net spin of 1/2 for each V(TCNE)$_x$ entity [7]. Each vanadium ion is coordinated to six cyano groups in a slightly distorted octahedral environment and the distribution of V–N bond lengths is small due to strong bonding between vanadium and TCNE [8]. The properties of V(TCNE)$_x$ make it potentially appealing for spintronics devices, e.g. spin valves. V(TCNE)$_x$ can be used as the soft ferromagnetic (FM) contact in a FM1/organic semiconductor/FM2 spin valve design [9]. Recently we proposed another spin valve design based on V(TCNE)$_x$, where it instead is used as organic semiconducting layer sandwiched between the two FM contacts [10]. This device make use of the fully spin-polarization and would operate in two different modes, either with two different FM contacts (one hard and one soft) or with two identical FM contacts.

Realization of such devices is complicated, however, and one of the main obstacles has been the preparation of the compound. When V(TCNE)$_x$ was first reported in 1991 [1], it was prepared in solution forming an insoluble, extremely air sensitive powder which contained both residual solvent molecules and residuals/by-products from the precursors (e.g. bis(benzene)vanadium, V(C$_6$H$_6$)$_2$ or vanadium hexacarbonyl, V(CO)$_6$). Presence of small amounts of contamination and/or disorder may affect both the magnetic properties [11,12] and the electronic properties [6] of the material negatively. A huge step forward was made when V(TCNE)$_x$ was prepared as thin films by a chemical vapor deposition (CVD) route [13,14]. Although the material was free from residual solvent molecules, such films still contained precursor residuals/by-products and oxygen-induced defects. Therefore an *in situ* method, based on CVD as well but compatible with any ultra-high vacuum system was developed to avoid oxidation problems and enable device fabrication [5]. This CVD-based method allowed for completely oxygen-free V(TCNE)$_x$ thin films to be fabricated, but the method produces magnets which still may contain small amounts of residuals from the bis(benzene)vanadium, V(C$_6$H$_6$)$_2$, precursor. In order to also get rid

* Corresponding author. Tel.: +46 13 28 1206; fax: +46 13 13 7568.
E-mail address: mafah@ifm.liu.se (M. Fahlman).

0379-6779/$ – see front matter © 2011 Elsevier B.V. All rights reserved.
doi:10.1016/j.synthmet.2011.06.031

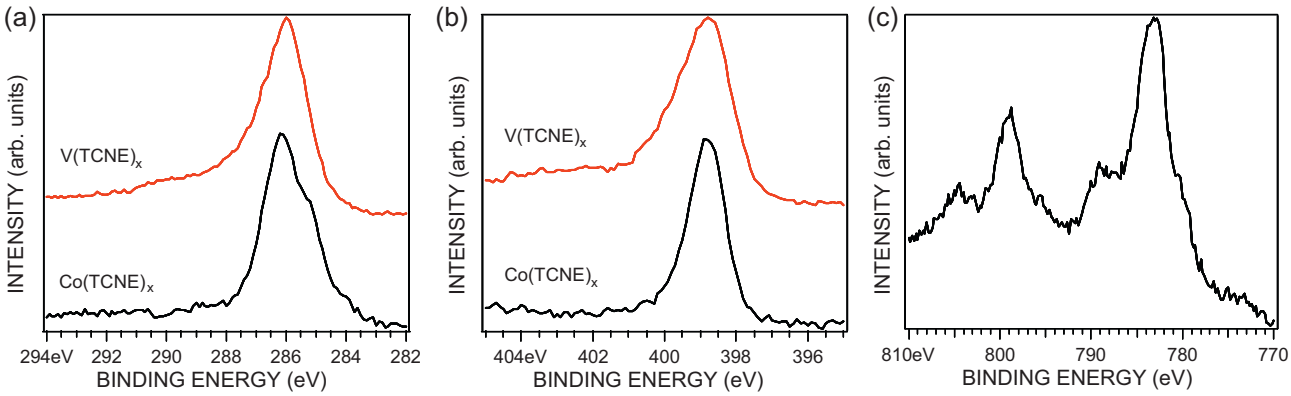

Fig. 1. Core level spectra of $Co(TCNE)_x$ and $V(TCNE)_x$. (a) C(1s), (b) N(1s), and (c) Co(2p).

of the precursor residuals an additional method, based on physical vapor deposition (PVD), was developed which results in oxygen-free $M(TCNE)_x$, neither containing residual solvent nor precursors (or by-products thereof) [15] since only pure metals and TCNE are used in the preparation process. The PVD process produces films more resistant to oxidation, but the outermost surface of $V(TCNE)_x$ films will always be highly reactive due to the V^{2+} sites present. Hence, though $V(TCNE)_x$ has been developed to the point where it is an interesting material for pursuing research on device physics, its commercial potential will depend on the effectiveness of sealing the devices from atmospheric contaminants (i.e. water and oxygen).

Substituting V^{2+} by a less reactive ion would greatly enhance the viability of using the hybrid organic magnets in devices, but few alternatives show RT magnetic ordering. In order to try to develop an understanding on what are the key design criteria for achieving critical temperatures above RT, we have begun to synthesize and study $M(TCNE)_x$ films that *do not* show RT magnetic ordering and comparing their chemical and electronic structure with that of $V(TCNE)_x$. $Fe(TCNE)_x$ and $Co(TCNE)_x$ were selected due their low critical temperatures, $T_C \sim 121$ K and $T_C \sim 44$ K respectively (values derived from their powder forms) [2]. We have shown in a previous paper that the HOMO of $Fe(TCNE)_x$ is mainly localized on $TCNE^-$ units in contrast to the case of $V(TCNE)_x$ and that the crystal field parameter of $Fe(TCNE)_x$, $10Dq \sim 0.6$ eV [16], also differs as compared to $V(TCNE)_x$ where $10Dq \sim 2.3$ eV [17]. The weaker crystal field parameter and the drastically different frontier valence electronic structure was proposed to explain the substantially lower magnetic ordering temperature of $Fe(TCNE)_x$ as compared to $V(TCNE)_x$. Herein, we present the first study on the electronic structure of $Co(TCNE)_x$, using a variety of photoemission and X-ray absorption techniques. The results are compared with the previously results on $V(TCNE)_x$ and $Fe(TCNE)_x$.

2. Experimental

Thin films of $Co(TCNE)_x$ were prepared on Au substrates at room temperature by a method based on physical vapor deposition. The base pressure of the preparation chamber was 10^{-9} mbar and the pressure upon $Co(TCNE)_x$ preparation was $\sim 5 \times 10^{-8}$ mbar. Studies were performed *in situ* using photoelectron spectroscopy (PES), near edge X-ray absorption fine structure (NEXAFS) and resonant photoelectron spectroscopy (RPES) at beamline D1011 of the MAX-II storage ring at the synchrotron radiation facility MAX-lab in Lund, Sweden. The (front) end-station is equipped with a Scienta SES electron analyzer and has a custom-built micro-channel plate (MCP) detector for electron yield measurements (NEXAFS). An incident angle $\theta = 45^\circ$ of the photon beam relative to the sample normal was used for all types of measurements. The backgrounds are not removed from the NEXAFS or the RPES spectra, neither the second order light nor the spectator decay contributions to the RPES spectra (but those contributions are indicated in the spectra).

Additional PES measurements were performed in our home laboratory by a Scienta® ESCA 200 spectrometer. X-ray photoelectron spectroscopy was performed using monochromatized Al(Kα) X-rays at $h\upsilon = 1486.6$ eV. The base pressure of the system was in the 10^{-9} mbar range. The $Co(TCNE)_x$ thin films were prepared under the same conditions in the home laboratory as in MAX-lab.

3. Results and discussion

The stoichiometry of $Co(TCNE)_x$ was estimated from the XPS wide scan, using atomic sensitivity factors which suggested about two TCNE molecules per cobalt ion. Upon PES, NEXAFS and RPES, no oxygen was present (to the detection limit of the measurements), confirming oxygen-free $Co(TCNE)_x$. The C(1s) core level of $Co(TCNE)_x$ and $V(TCNE)_x$, respectively, see Fig. 1a, are located at roughly the same position (286.0 and 286.2 eV, respectively). The C(1s) peak of $V(TCNE)_x$ has a shake-up feature at the higher binding energy side of the main peak, which is absent for $Co(TCNE)_x$ (as well as for $Fe(TCNE)_x$ [16]). This indicates that the LUMO of $Co(TCNE)_x$ (and $Fe(TCNE)_x$) is modified as compared to the $V(TCNE)_x$ counterpart, which suggests the HOMO to be modified as well. There is an asymmetry at the low binding energy side of C(1s) of $Co(TCNE)_x$ which also is present for C(1s) of $Fe(TCNE)_x$ [16]. This low-binding energy feature of C(1s) has been seen in low-quality $V(TCNE)_x$ films, where it is attributed to a bonding defect: vanadium bonding to vinyl sites of TCNE instead of the cyano ligands [15]. Hence the presence of the C(1s) low-binding energy feature suggests a more disordered film growth for $Co(TCNE)_x$ (and for $Fe(TCNE)_x$ [16]) as compared to $V(TCNE)_x$.

The N(1s) core level of $Co(TCNE)_x$ and $V(TCNE)_x$, see Fig. 1b, are located at the same position, i.e. at 398.8 eV. As for C(1s), N(1s) of $Co(TCNE)_x$ (and of $Fe(TCNE)_x$ [16]) lacks the shake-up feature, an indication of modified LUMO and HOMO as compared to $V(TCNE)_x$. However, the most striking difference between N(1s) of $Co(TCNE)_x$ and $V(TCNE)_x$ is that N(1s) of $V(TCNE)_x$ is much broader than N(1s) of $Co(TCNE)_x$. We speculate that this is due to that cobalt preferentially bonds to the vinyl groups of TCNE instead of the cyano groups (as in $V(TCNE)_x$), since C(1s), but not N(1s) is broadened as compared to pristine TCNE. Given that the C(1s) and N(1s) of $Co(TCNE)_x$ (and of $Fe(TCNE)_x$ [16]) are very different as compared to the corresponding C(1s) and N(1s) core level peaks of $V(TCNE)_x$ [5], it indicates the physical and chemical environment to be different in the three compounds.

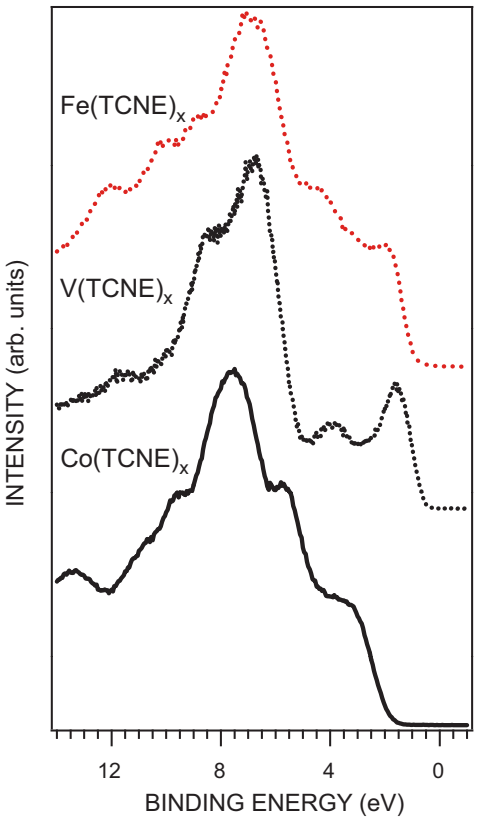

Fig. 2. Valence region spectra of $Co(TCNE)_x$, $V(TCNE)_x$ and $Fe(TCNE)_x$, respectively, taken at 100 eV. The intensity is normalized with respect to the main peak at ~7 eV.

Co(2p), depicted in Fig. 1c, is shifted towards higher binding energy as compared to pristine cobalt and has a feature on each of the higher binding energy sides of the $Co(2p_{1/2})$ and $Co(2p_{3/2})$ peaks, respectively, confirming reaction with TCNE. The shift towards higher binding energy for Co(2p) and shift towards lower binding energy for C(1s) and N(1s) as compared to pristine cobalt and TCNE suggests charge transfer from cobalt to TCNE and based on the stoichiometry estimation, cobalt is tentatively assigned to Co^{2+}.

The valence region spectra of $Co(TCNE)_x$, $Fe(TCNE)_x$ and $V(TCNE)_x$ are depicted in Fig. 2. The most intense peak of $Co(TCNE)_x$ is located at ~7.5 eV and there are at least two peaks riding on its higher binding energy side slope. A third feature is present at 13.5 eV. At the lower binding energy side of the main peak there is one peak at 5.5 eV and a broad shoulder extending between 4.5 and 2.0 eV containing the density of states from the HOMO of $Co(TCNE)_x$. There is no sharp Fermi edge visible in the spectrum and thus no evidence for metallic cobalt in the thin film. Like $Co(TCNE)_x$, $Fe(TCNE)_x$ has three features on the high binding energy side of the main valence region peak. The frontier occupied valence region of $Fe(TCNE)_x$ has also three distinct features, the first and strongest feature at 4.5 eV which originates from Fe(3d), a second feature at 3.0 eV and a third feature at 1.7 eV, representing the state derived from the HOMO of neutral TCNE and the $TCNE^-$ singly occupied molecular orbital (SOMO), respectively [16]. Whereas the same features are present in the valence spectra of $Fe(TCNE)_x$ and $Co(TCNE)_x$, even if the binding energies and relative intensities slightly vary, the frontier electronic structure of $V(TCNE)_x$ is significantly different. For $V(TCNE)_x$, there are three features present at the low binding energy side of the main peak at 6.5 eV, namely the former TCNE HOMO at 3.5 eV, the SOMO of $TCNE^-$ at 1.5 eV and a hybridized V(3d) – TCNE(π) state at 1 eV [5,17].

In order to determine the origin of the features in the $Co(TCNE)_x$ valence band spectrum, and in particular the origin of the frontier electronic state, resonant photoemission spectroscopy (RPES) was carried out at the C K-edge, N K-edge and Co L-edge, see Figs. 3a, 4a and 5a, respectively. RPES allows for elemental specific analysis of the valence electronic structure and is performed by sweeping the photon energy in discrete steps over the respective absorption edge while monitoring the electrons emitted from the valence region. When the RPES show resonating behaviour originating from participator decay it is possible to determine the origin of the features and peaks in the $Co(TCNE)_x$ valence band spectrum in Fig. 2. There are also additional contributions from competing processes, such as spectator decay (peak binding energy increases linearly with increased photon energy), and more complex Auger-type decay which appears like an added background [18]. Furthermore there are core level peaks originating from core-ionization by second order light that disturb the C and N K-edge spectra, particularly the N K-edge. Those peaks move towards lower binding energy as the photon energy is increased and are represented by red bars in the respective RPES spectra.

The C K-edge RPES of $Co(TCNE)_x$, see Fig. 3a, was obtained by sweeping the photon energy in discrete steps from 280.0 to 289.0 eV to hit the features in the corresponding C K-edge NEXAFS spectrum, depicted in Fig. 3b. The spectra with photon energy 280.0 and 282.0 eV are taken below the absorption onset seen in the C K-edge NEXAFS spectrum and hence no resonating behaviour is observed. For photon energy 284.2 eV the onset has been passed, but there are only very weak resonant contributions in the RPES spectrum. For 285.1 eV, however, there is a slight increase in the background, especially at higher binding energies, and hence some enhancement in the resonance contribution to the signal. The maximum of the main absorption peak is located at 286.3 eV and for this photon energy strong resonating behaviour is apparent for several peaks, especially for the one located at ~7.5 eV, hence originating from TCNE-derived orbitals. This is not surprisingly since TCNE has about ten molecular orbitals in this region [19,20] and both $V(TCNE)_x$ and $Fe(TCNE)_x$ have TCNE-derived states at approximately this position. There is a relative flattening out of the region between 6 and 2 eV, suggesting a resonant enhancement of the low binding energy shoulder (4.5–2.0 eV), increasing its intensity compared to the peak at 5.5 eV. This suggests that the low binding energy shoulder contains contributions from TCNE-derived orbitals. For the second largest absorption peak, located at 287.5 eV, there is still strong enhancement of the resonance at 7.5 eV, however it is now slightly hidden by resonating features at higher binding energies. Finally, for the spectrum taken at 289.0 eV there is a resonating feature at 13.5 eV, hence originating from TCNE but mainly this spectrum is dominated by a background which comes from Auger type processes.

The N K-edge RPES and NEXAFS spectra, presented in Fig. 4a and b, were obtained in the same way as the C K-edge counterparts. For the N K-edge RPES taken at 392.0 and 395.0 eV there is no resonating behaviour as they both are taken below the N K-edge onset. An increase in background and hence some resonant behaviour is seen for the RPES spectrum taken at 396.5 eV since it is performed at the (weak) N K-edge onset. At the absorption maximum which is located at 398.9 eV there are two features resonating around 9 and 7 eV, indicating those features in the valence spectrum to be TCNE-derived. There is strong background at higher binding energies which could be attributed to Auger processes. Similar to the C K-edge, there is a relative flattening out of the region between 6 and 2 eV, suggesting a resonant enhancement of the low binding energy shoulder as compared to the feature at 5.5 eV. This supports the assignment of the low binding energy shoulder to TCNE-derived orbitals. For 400.1 eV photon energy, which is related to the second maximum absorption peak, there is a strong background contribu-

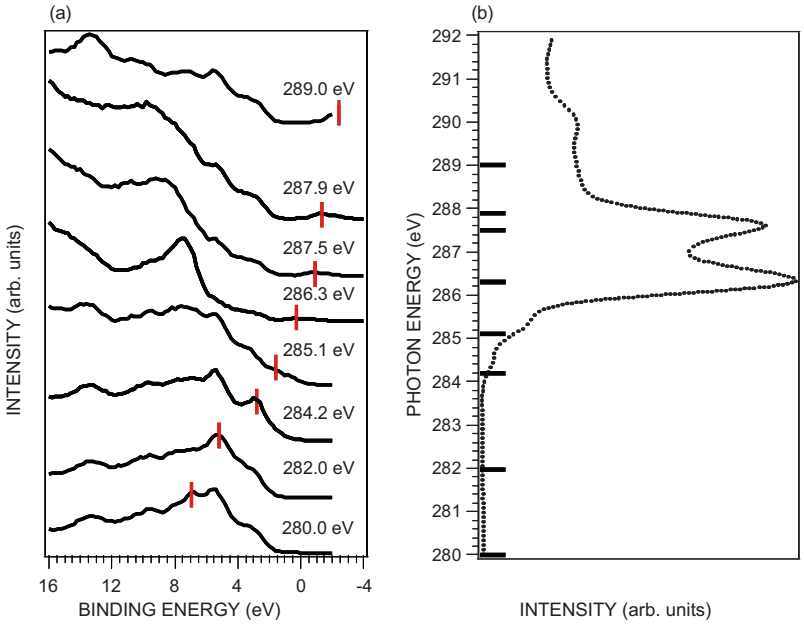

Fig. 3. (a) RPES spectra taken by sweeping the photon energy in discrete steps over the C K-edge of $Co(TCNE)_x$. The second order light-induced C(1s) core level peak features have not been removed from the RPES spectra but are marked with bars. (b) The corresponding C K-edge NEXAFS spectrum. The RPES photon energies are represented by bars.

tion and a flattening out of the area between 6 and 2 eV. There may also be a spectator decay process moving across and disturbing the N K-edge spectra. This possible contribution is marked with blue bars in Fig. 4.

The Co L-edge RPES spectrum and corresponding NEXAFS spectrum are shown in Fig. 5a and b. The second order light contribution of the RPES spectra is very weak and does not even affect the spectra, unlike the case for the C and N K-edges. The spectra at 770.0 and 772.1 eV are taken off-resonance and therefore no resonance enhancement is seen. The Co L-edge absorption maximum is located at 777.7 eV and it gives rise to strong resonating behaviour for the peak at ~5 eV, suggesting it to be Co(3d)-derived. At 781.5 eV the X-ray absorption peak maximum has been passed and the contributions to the spectrum originate from background and hence Auger processes.

Founded on the combined PES and RPES results, the main peak at 7.5 eV in the $Co(TCNE)_x$ valence band spectrum in Fig. 2 is derived from TCNE. Its shoulder on the lower binding energy side, at ~5 eV, originates from Co(3d) and the lowest binding energy feature centred between 4.5 and 2.0 eV is derived from TCNE orbitals (assigned as former HOMO and $TCNE^-$ SOMO). Thus, the results show that the valence region of $Co(TCNE)_x$ is more similar to the $Fe(TCNE)_x$ counterpart as compared to $V(TCNE)_x$ since the lowest binding energy feature of both $Co(TCNE)_x$ and $Fe(TCNE)_x$ in the valence spectra are

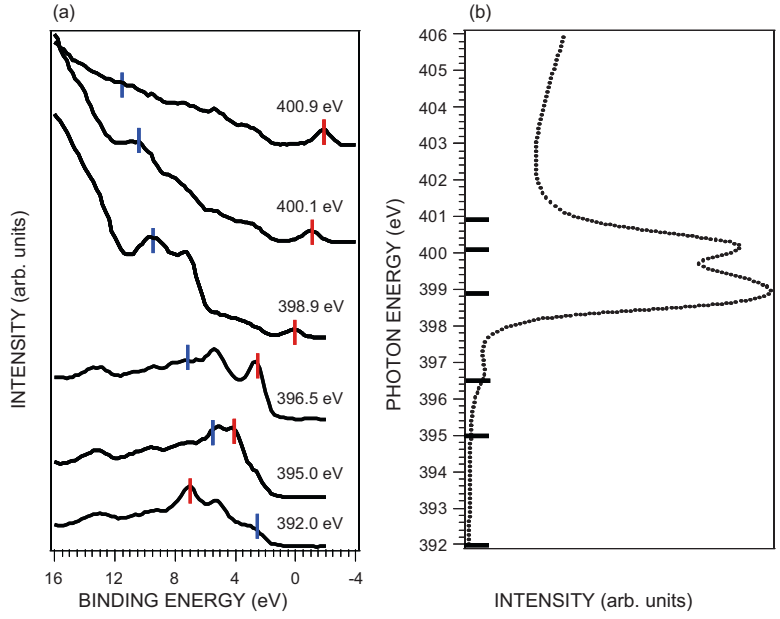

Fig. 4. (a) RPES spectra taken by sweeping the photon energy in discrete steps over the N K-edge of $Co(TCNE)_x$. The second order light-induced N(1s) core level peak features have not been removed from the RPES spectra but are marked with red bars. The possible spectator decay is marked by blue bars in the spectra. (b) The corresponding N K-edge NEXAFS spectrum. The RPES photon energies are represented by bars.

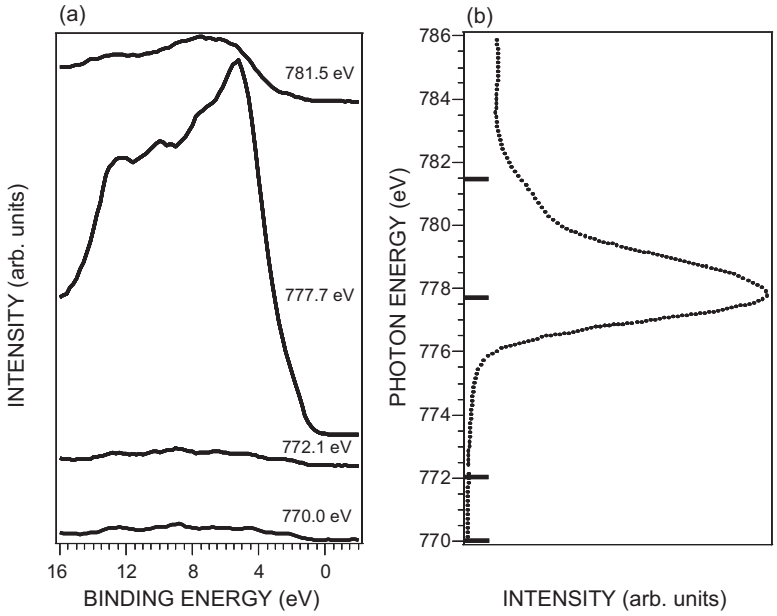

Fig. 5. (a) RPES spectra taken by sweeping the photon energy in discrete steps over the Co L-edge of $Co(TCNE)_x$. The second order light related features are very weak and are not removed or marked in the RPES spectra. (b) The corresponding C K-edge NEXAFS spectrum. The RPES photon energies are represented by bars.

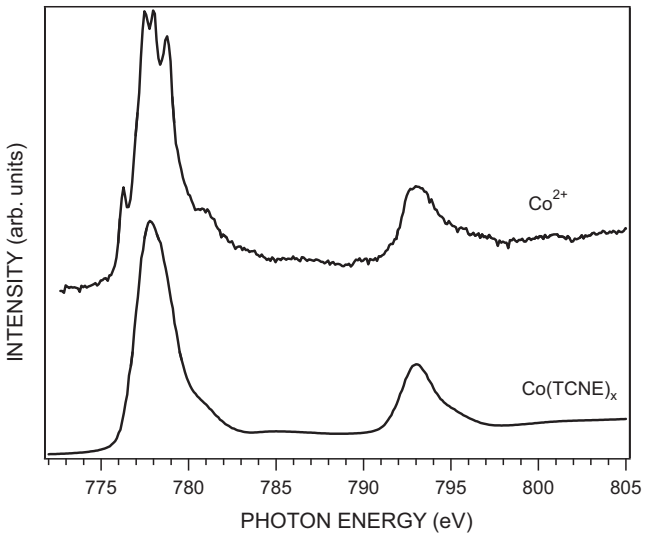

Fig. 6. Co L-edge NEXAFS spectra of $Co(TCNE)_x$ and Co^{2+} (cobalt in Co-doped TiO_2, octahedral $10Dq = 1.1$ eV).

TCNE-derived in contrast to $V(TCNE)_x$ where it is mainly V(3d)-derived.

In Fig. 6, Co L-edge NEXAFS spectrum of $Co(TCNE)_x$ is depicted together with a reference spectrum of Co^{2+} obtained at the I1011 beam line, MAX-lab. The position of the Co L-edge in $Co(TCNE)_x$ is in good agreement with the position of Co^{2+}, further strengthening the suggested cobalt valency of 2+. The fact the Co L-edge of $Co(TCNE)_x$ lacks fine structure is most probably related to disorder, since there could be a distribution of cobalt ions in different bonding arrangements (with varying ligand field strength and significant distortion away from the octahedral arrangement as observed in $V(TCNE)_x$). If there would be a well-defined cobalt species, there should be some multiplet structure, also for weak (in the extreme case zero) crystal field splitting. Since $Co(TCNE)_x$ does not show any pronounced fine structure it is difficult to make a reliable estimate of the crystal field using ligand field multiplet calculations, like the ones that were performed for the $V(TCNE)_x$ V L-edge [17] and for the $Fe(TCNE)_x$ Fe L-edge [16]. However, from the lack of shoulders it seems that that the crystal field is very weak (much smaller than 1 eV, since the width of the multiplet distribution scales with the crystal field strength), which can be compared with $V(TCNE)_x$ ($10Dq = 2.3$ eV) and $Fe(TCNE)_x$ ($10Dq = 0.6$ eV). Based on the combined PES and NEXAFS results we speculate that TCNE binds differently to cobalt as compared to vanadium, i.e. most likely not solely in an octahedral arrangement. The PES data suggests that cobalt preferentially binds to the vinyl – instead of the cyano groups as in $V(TCNE)_x$, since C(1s), but not N(1s), of $Co(TCNE)_x$ is broadened as compared to pristine TCNE. Studies of other π-conjugated systems with vinyl- and cyano groups forming interfaces with transition metal atoms have shown that the transition metal preferentially bond to the cyano group but that the vinyl group also is an option [21]. We speculate that the bonding environment in $Co(TCNE)_x$ is disordered and that cobalt preferentially binds to vinyl carbons instead of cyano carbons. The different physical environment and the large amount of disorder explain the poor magnetic properties of $Co(TCNE)_x$. However, from these results it is not possible to say if the main reason for the low critical temperature of $Co(TCNE)_x$ is due to the disordered nature of the compound, the different bonding interaction and hence different frontier electronic structure, or if it is a combination of both.

4. Conclusions

In order to find the key design criteria for RT magnetic ordering we have started to study the electronic and chemical structure of low critical temperature $M(TCNE)_x$ magnets and comparing them with $V(TCNE)_x$. Herein, thin films of $Co(TCNE)_x$, $x \sim 2$, were prepared by a PVD-based process and studied with PES, NEXAFS and RPES. The results suggest that the PVD-fabricated $Co(TCNE)_x$ thin films contain large amounts of local bonding disorder in contrast to PVD-fabricated $V(TCNE)_x$ which can be grown virtually defect free. From the N(1s) spectrum we see that there is very weak (or non-existing) interaction between the nitrogen and cobalt. We speculate that the cobalt binds to the vinyl groups instead of the cyano groups of TCNE leading to a variable bonding arrangement which deviates from octahedral. This is further strengthen by the fact that the crystal field splitting is very weak (simulations were not pos-

sible since no multiplets could be resolved). The HOMO of both $Co(TCNE)_x$ and $Fe(TCNE)_x$ are TCNE-derived while the states originating from Co(3d) and Fe(3d) respectively are located at higher binding energies, in stark contrast to the valence region of $V(TCNE)_x$ where the HOMO is mainly V(3d)-derived. The similarities in terms of electronic and chemical structure of PVD-fabricated $Co(TCNE)_x$ and $Fe(TCNE)_x$, dictated by the as compared with $V(TCNE)_x$ different interaction of the metal 3d orbitals with the π-orbitals of TCNE, are in line with their significantly lower Curie temperatures as compared to the RT magnetic ordering of $V(TCNE)_x$.

Acknowledgements

The Surface Physics and Chemistry division is supported by the Swedish Research Council (project grant) and the Knut and Alice Wallenberg Foundation (equipment).

References

[1] J.M. Manriques, G.T. Yee, R.S. McLean, A.J. Epstein, J.S. Miller, Science 252 (1991) 1415.
[2] J. Zhang, J. Ensling, V. Ksenofontov, P. Gütlich, A.J. Epstein, J.S. Miller, Angew. Chem. Int. Ed. 37 (1998) 657.
[3] D. de Caro, M. Basso-Bert, H. Casellas, M. Elgaddari, J.-P. Savy, J.-F. Lamère, A. Bachelier, C. Faulmann, I. Malfant, M. Étienne, L. Valade, C. R. Chim. 8 (2005) 1156.
[4] V.N. Prigodin, N.P. Raju, K.I. Pokhodnya, J.S. Miller, A.J. Epstein, Adv. Mater. 14 (2002) 1230.
[5] C. Tengstedt, M.P. de Jong, A. Kanciurzewska, E. Carlegrim, M. Fahlman, Phys. Rev. Lett. 96 (2006) 057209.
[6] E. Carlegrim, A. Kanciurzewska, M.P. de Jong, C. Tengstedt, M. Fahlman, Chem. Phys. Lett. 452 (2008) 173.
[7] J.B. Kortright, D.M. Lincoln, R.S. Edelstein, A.J. Epstein, Phys. Rev. Lett. 100 (2008) 257204.
[8] D. Haskel, Z. Islam, J. Lang, C. Kmety, G. Srajer, K.I. Pokhodnya, A.J. Epstein, J.S. Miller, Phys. Rev. B 70 (2004) 054422.
[9] J.-W. Yoo, C.-Y. Chen, H.W. Jang, C.W. Bark, V.N. Prigodin, C.B. Eom, A.J. Epstein, Nat. Mater. 9 (2010) 638.
[10] E. Carlegrim, Y. Zhang, F. Li, X. Liu, M. Fahlman, Org. Electron. 11 (2010) 1020.
[11] K.I. Pokhodnya, D. Pejakovic, A.J. Epstein, J.S. Miller, Phys. Rev. B 63 (2001) 174408.
[12] M.S. Thorum, K.I. Pokhodnya, J.S. Miller, Polyhedron 25 (2006) 1927.
[13] K.I. Pokhodnya, A.J. Epstein, J.S. Miller, Adv. Mater. 12 (2000) 410.
[14] D. de Caro, M. Basso-Bert, J. Sakah, H. Casellas, J.-P. Legros, L. Valade, P. Cassoux, Chem. Mater. 12 (2000) 587.
[15] E. Carlegrim, A. Kanciurzewska, P. Norblad, M. Fahlman, Appl. Phys. Lett. 92 (2008) 163308.
[16] P. Bhatt, E. Carlegrim, A. Kanciurzewska, M.P. de Jong, M. Fahlman, Appl. Phys. A 95 (2009) 131.
[17] M.P. de Jong, C. Tengstedt, A. Kanciurzewska, E. Carlegrim, W.R. Salaneck, M. Fahlman, Phys. Rev. B 75 (2007) 064407.
[18] P.A. Brühwiler, O. Karis, N. Mårtensson, Rev. Mod. Phys. 74 (2002) 703.
[19] V.G. Zakrzewski, O. Dolgounitcheva, J.V. Ortiz, J. Chem. Phys. 105 (1996) 5872.
[20] K.N. Houk, L.L. Munchausen, J. Am. Chem. Soc. 98 (1976) 937.
[21] M. Fahlman, W.R. Salaneck, S.C. Moratti, A.B. Holmes, J.L. Brédas, Chem. Eur. J. 3 (1997) 286.